DOI: 10.6060/mhc256698k

On the Photosensitized Formation of Singlet Oxygen by Water-Soluble Bacteriochlorin Derivative – Tetrahydroporphyrin-Tetratosylate in Aerated Aqueous Solutions

Alexander A. Krasnovsky Jr.,[a,c@] Anton S. Benditkis,[a,c] Anton S. Kozlov,[a] Maria V. Kishalova,[b] and Alexey V. Lyubimtsev[b]

[a]*A.N. Bach Institute of Biochemistry, Federal Research Center «Fundamentals of Biotechnology», the Russian Academy of Sciences, 119071 Moscow, Russian Federation*
[b]*Ivanovo State University of Chemistry and Technology, 153000 Ivanovo, Russian Federation*
[c]*Moscow Pedagogical State University (MPGU), 119991 Moscow, Russian Federation*
[@]*Corresponding author E-mail: phoal@mail.ru*

Dedicated to Corresponding Member of the Russian Academy of Sciences G. N. Vorozhtsov on the occasion of his 90th Anniversary

The synthetic water-soluble photosensitizer, tetrahydroporphyrin tetratosylate (THPTS), which is a 1:5 molar mixture of N-methylated meso-tetra(3-pyridyl) derivatives of chlorin and bacteriochlorin, is known as an effective photosensitizer for antitumor and antimicrobial photodynamic therapy (PDT). Due to the intense infrared absorption band (760 nm) it is also suitable for the detection and treatment of subcutaneous tumors. In recent years, the synthesis of this compound has been optimized and simplified, making it affordable for widespread medical applications. In the present study, we investigate the photogeneration of singlet molecular oxygen ($^1O_2$) of the newly synthesized THPTS as well as its absorption spectra and fluorescence parameters in aerated ethanol, D_2O, and H_2O. Singlet oxygen was studied using both detection of luminescence at 1270 nm and $^1O_2$ chemical trapping by 1,3-diphenylisobenzofuran (DPIBF). It was found that the bacteriochlorin component of THPTS generates $^1O_2$ with almost equal quantum yield (Φ_Δ = 0.45–0.65) in ethanol and aqueous solutions. This result disagrees with the prior data of Riyad et al. (J. Phys. Chem. B, 2014, 118, 11646–11658) who could not detect $^1O_2$ in aqueous THPTS solutions and proposed that THPTS loses an ability to photosensitize $^1O_2$ formation in water and living systems. Based on this conclusion, the authors suggested that photodynamic action photosensitized by THPTS is solely due to the free-radical Type I mechanism. Our results indicate that $^1O_2$ is efficiently generated by THPTS in water, therefore, the Type II mechanism might well be the primary step of the THPTS photodynamic action in both aquatic and non aquatic environments. The reasons for the discrepancy in results of our and Shastak's groups are discussed.

Keywords: Bacteriochlorin, tetrahydroporphyrin-tetratosylate, singlet oxygen, photosensitization, aqueous medium.

О фотосенсибилизации образования синглетного кислорода водорастворимым производным бактериохлорина – тетрагидропорфирин-тетратозилатом в аэрированных водных растворах

А. А. Красновский мл.,[a,c@] А. С. Бендиткис,[a,c] А. С. Козлов,[a] М. В. Кишалова,[b] А. В. Любимцев[b]

[a]*Институт биохимии им. А.Н. Баха, ФИЦ Биотехнологии РАН, 119071 Москва, Российская Федерация*
[b]*ФГБОУ ВО Ивановский государственный химико-технологический университет, 153000 Иваново, Российская Федерация*
[c]*Московский педагогический государственный университет (МПГУ), 119991 Москва, Российская Федерация*
[@]*E-mail: phoal@mail.ru*

Синтетический водорастворимый фотосенсибилизатор, «тетрагидропорфирин-тетратозилат» (THPTS), являющийся 1/5 молярной смесью тозилатов N-метилированных мезо-тетра(3-пиридил)хлорина и мезо-тетра(3-пиридил)бактериохлорина, известен как эффективный противоопухолевый и противомикробный фотосенсибилизатор для ФДТ, который, благодаря интенсивной инфракрасной полосе поглощения (760 нм), пригоден в том числе, для обнаружения и лечения подкожных новообразований. В последние годы синтез этого соединения был оптимизирован и упрощен, что сделало его доступным по стоимости для широкого применения в медицине. В настоящей работе проведено исследование фотогенерации синглетного молекулярного кислорода ($^1O_2$), а также спектры поглощения и параметры флуоресценции вновь синтезированного THPTS в этаноле, D_2O и H_2O. Синглетный кислород регистрировали по инфракрасной люминесценции при 1270 нм и по окислению химической ловушки синглетного кислорода 1,3-дифенилизобензофурана (DPIBF). Обнаружено, что бактериохлориновый компонент THPTS фотосенсибилизирует $^1O_2$ с практически одинаковым квантовым выходом (Φ_Δ = 0,45–0,65) во всех использованных средах. Эти результаты противоречат данным работы Ryiad et al. (J. Phys. Chem. B 2014, 118, 11646–11658), которые не обнаружили $^1O_2$ в водных растворах THPTS, и поэтому предположили, что в водной среде и в живых организмах THPTS теряет способность генерировать $^1O_2$ и его фотосенсибилизирующее действие – исключительно результат радикальной реакции типа I. Наши данные показывают, что THPTS одинаково эффективно генерирует $^1O_2$ как в водных средах, так и этаноле, поэтому при фотодинамическом действии THPTS механизм типа II должен быть более вероятным. Обсуждаются причины расхождения результатов.

Ключевые слова: Бактериохлорин, тетрагидропорфирин-тетратозилат, синглетный кислород, фотосенсибилизация, водная среда.

Introduction

The synthesis of effective photosensitizers for photodynamic therapy (PDT) of tumors and infectious diseases is one of the most actively developing fields of modern photomedical research. Presently, great attention is paid to derivatives of chlorophyll *a* and bacteriochlorophyll *a*, the latter being the major pigment of photosynthetic bacteria.[1-6] The main absorption maximum of bacteriochlorophyll *a* is in the dark red region (740–760 nm) – that is, at wavelengths that penetrate deeper into living tissues than the red light (650–670 nm) absorbed by chlorophyll.[1-4] An ability of bacteriochlorophylls *a*, *b*, their magnesium-free analogs – bacteriopheophytins and synthetic *meso*-tetraphenylbacteriochlorin to photosensitize phosphorescence of singlet oxygen at 1270 nm in aerated tetrachloromethane has been observed in pioneering papers.[7-10] Later similar phosphorescence was detected in other organic solvents and aqueous dispersions of detergent micelles (see recent mini-review[11]).

In 2002, a new bacteriochlorin-based photosensitizer has been synthesized. This compound termed "tetrahydroporphyrin-tetratosylate" (THPTS) showed tropism to neoplasms of various natures and high anticancer and antimicrobial activities under action of dark red light at 760 nm ([12-14] and refs therein). Chemically this compound was a mixture of water-soluble tetratosylate salts of N-methylated *meso*-tetra(3-pyridyl)bacteriochlorin and N-methylated *meso*-tetra(3-pyridyl)chlorin[12] with molar ratio 5/1 (Scheme 1).

In 2011–2012 Dr. Shastak brought this compound to Krasnovsky's lab in Moscow for analysis. It was found that both components emitted fluorescence and generated singlet oxygen in aerated ethanol and water. The quantum yields of $^1O_2$ generation by the bacteriochlorin component of THPTS estimated using $^1O_2$ trapping by 1,3-diphenylisobenzofuran (DPIBF) were 0.5 in ethanol and 0.4 in water with 0.2 M SDS, which was added for solubilization of the trap. These results were reported in several groups with a proposal to develop a low-cost synthesis of this compound, which would allow application THPTS in PDT.

Soon (starting from 2013–2014), the groups of Dr. Koifman (Ivanovo) and Dr. Lukyanetz (Moscow) reported different synthetic and purification procedures.[15-19] In particular, Dudkin *et al*. using 9,10-dimethylantracene (DMA) as a trap, obtained that the quantum yields of singlet oxygen generation by free base and water-soluble derivatives of THPTS are equal to 0.5 in aerated methanol.[17] This value is close to the Φ_Δ previously obtained by our group in ethanol and water with 0.2 M SDS. The results suggested that the photodynamic action of THPTS is due to photogeneration of $^1O_2$ by this photosensitizer.

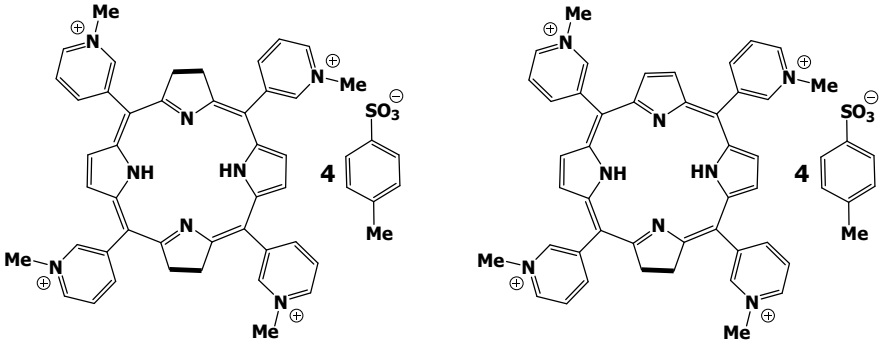

Scheme 1. Chemical structures of bacteriochlorin (left) and chlorin (right) components of THPTS and the counterion (tosylate).

More recently, Riyad *et al*.[20] questioned this thesis. According to their data, THPTS loses an ability to photosensitize $^1O_2$ in aqueous environment although it efficiently ($\Phi_\Delta = 0.75$) generated $^1O_2$ in aerated acetonitrile. They proposed that in living cells and tissues, THPTS works via the Type I mechanism due to primary reduction of the triplet THPTS by electron donors in the cellular environment. Similar mechanism was assumed to be valid for a group of other photosensitizers with low energies of the triplet states (see[20] for refs). Natural bacteriochlorophylls of bacterial photosynthetic cells might also belong to this group. Recently, keeping this in mind, we have experimentally studied $^1O_2$ formation by bacteriochlorophyll *a* in organic and aqueous environment. It was obtained using a chemical trapping method and detection of phosphorescence at 1270 nm that bacteriochlorophyll efficiently generates $^1O_2$ in organic solvents and aqueous micellar dispersions as well.[11] To our knowledge, similar systematic studies of singlet oxygen generation by THPTS in water has never been published. Indeed, Riyad et al. could not detect singlet oxygen in aqueous solutions of THPTS[20]. Our group, as mentioned above, got an opposite result but it has been reported only in oral form at different local meetings.

Recently, Lyubimtsev *et al*.[18,19] significantly simplified the synthetic procedure. This reduced the cost of the final product and facilitated production of it in larger quantities, necessary for experiments on cell models, laboratory animals and humans.

The present work is aimed at studying abilities of synthetic THPTS to photosensitize singlet oxygen formation in aqueous environment and organic solvent (ethanol). For investigation of $^1O_2$, both trapping of singlet oxygen by DPIBF and detection of $^1O_2$ phosphorescence at 1270 nm were applied. THPTS is readily solubilized in ethanol, water and D_2O. Pigment molecules were found to generate singlet oxygen in all solvents including water with almost equal efficiencies. The data indicate that the investigated pigments are promising photosensitizers for antitumor and antimicrobial PDT, with the Type II (via singlet oxygen) primary mechanism of action.

Experimental

Materials

Tetrahydroporphyrin-tetratosylate (THPTS) studied in the present work was synthesized using the methods described in papers.[18,19] Like the prototype obtained from Shastak, it was a mixture (5:1) of bacteriochlorin and chlorin derivatives (Scheme 1). All reagents and solvents were commercially available. All synthesized pigments were analyzed using ^1H NMR, UV/Vis and MS (MALDI TOF) spectrometry. The solvents were ethanol (96%, rectified "Lux"-grade, Donskoy LLC, Russia), deuterium oxide, >99.5%, Chemical Line LLC, Russia), and water (bidistilled, from A.N. Bach Institute of Biochemistry, FRC of Biotechnology RAS, Moscow).

Absorption and fluorescence measurements

The absorption spectra were measured using the SF-56 spectrophotometer (LOMO-Spektr LLC, Russia) in quartz cells with an optical path of 10 and 5 mm. Fluorescence spectra were measured on a computerized fluorimeter Perkin Elmer MPF-44B. Fluorescence was detected at the right angle to the excitation beam. Spectral width of the monochromator slits corresponded to 3 nm. Spectral data were processed and analyzed using Microsoft Excel spreadsheets. The fluorescence quantum yields (Φ_f) were determined using *meso*-tetrakis(*p*-sulfonatophenyl)porphyrin tetra sodium salt (TPPS) in ethanol and aqueous as a reference. The Φ_f of the reference compound is known to be of 0.085±0.005.[21,22]

Photosensitizing activity

As a measure of the pigment photosensitizing activity, the values of the quantum yields (Φ_Δ) of photosensitized generation of singlet oxygen were employed. For detection of singlet oxygen, chemical trapping and detection of 1270 nm phosphorescence were applied. The main principles of the methods are illustrated by Scheme 2.

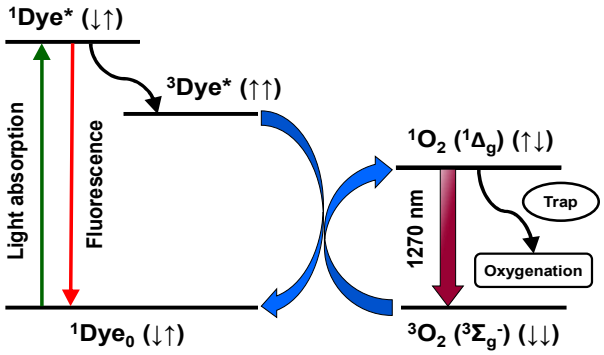

Scheme 2. Simplified energy diagram describing the mechanism of photosensitized formation of singlet oxygen and principles of $^1O_2$ detection via phosphorescence emission (1270 nm) and chemical trapping.

Trapping method

For singlet oxygen trapping, 1,3-diphenylisobenzofuran (DPIBF, >99%, Acros Organics, Belgium) was used. This trap has been known for several decades since the pioneering paper.[23] It has a single absorption band with a maximum at about 414 nm. When DPIBF reacts with singlet oxygen, colorless products are formed, therefore absorbance at 414 nm decreases. The rate of singlet oxygen production by dyes was calculated from the rate of reduction of DPIBF absorbance at 414 nm. The initial absorbance of DPIBF was 1±0.1 at 414 nm in a 10 mm quartz cell that corresponds to the DPIBF concentration of 42±4 μM (see additional details in[24,25]). The trap is insoluble in neat water and D_2O. A detergent sodium dodecyl sulfate (SDS) (Panreac Quimica SAU, Spain) (0.2 M) was applied for solubilization of DPIBF in aqueous media. Solubilization was carried out by adding concentrated solutions of DPIBF in acetone (for spectroscopy, Komponent-reaktiv LLC, Russia) to SDS dispersions in water or deuterium oxide, followed by shaking (1–2 min). The final concentration of acetone in the sample was about 3–5% (by volume). In ethanol, DPIBF formed stable solutions. In the SDS-water (or D_2O) mixtures stable DPIBF containing dispersions were formed. During irradiation and the measurement procedure no sedimentation of the trap occurred.[24,25] It is known that CMC (critical micelle concentration) for SDS is 0.008 M.[26,27] In the 0.2 M SDS dispersion, all detergent molecules are included in nanosize micelles (4–6 nm in diameter) with molecular weight of about 18 kD (62 molecules of SDS).[26] The p*H* is shifted to 7.5. Therefore, in the presence of 0.2 M SDS the molar concentration of micelles was $3.2 \cdot 10^{-3}$ M. Thus, there are 76 micelles per 1 trap molecule. In agreement with Poisson distribution, the probability that one micelle contains more than 1 DPIBF molecule is close to zero. As shown previously, the effective rate constant of the reaction of one DPIBF encapsulated

in a micelle is 2-fold greater compared to a solution of the trap in ethanol.[24]

The quantum yields were determined using a water-soluble TPPS as a reference compound, for which Φ_Δ is known to be 0.70±0.05.[24,28,29] A trap, DPIBF was solubilized in water by micelles of 0.2 M SDS. Samples were irradiated by monochromatic light from the excitation unit of the Perkin Elmer MPF-44B fluorimeter. THPTS was irradiated by dark red 760 nm light. For irradiation of TPPS green light of 510–515 nm was employed. In both cases, the exciting light was not absorbed by the trap. Thorlabs PM-100D meter with an S120VC measuring head was used to control power of the exciting radiation.

Detection of IR phosphorescence

IR phosphorescence of singlet oxygen (1270 nm), arises due to the energy transfer from triplet molecules of the photosensitizers (dyes) to oxygen molecules (Scheme 2). As a result, molecules of singlet oxygen ($^1\Delta_g$) appear which emit phosphorescence at 1270 nm. Phosphorescence was detected using a spectrometer recently assembled in Krasnovsky's laboratory (A.N. Bach Institute of Biochemistry, FRC of Biotechnology RAS, Moscow).[30] Pulsed LEDs with an emission band at 367 and 395 nm and a half bandwidth of 16 and 30 nm, respectively (Polironic LLC, Russia) were used as an excitation source. The pulse repetition rate was of 5–50 kHz, and the flash duration was of 1–2 μs. The LED radiation was focused into a spot with the diameter of 5 mm on the surface of quartz spectroscopic cells with studied solutions. Phosphorescence was recorded using a FEU-112 photomultiplier (Ekran Optical Systems, Russia) with the S-1 spectral response, cooled with liquid nitrogen vapor to –30 °C. The signal from the photomultiplier passed through a preamplifier to a photon counting board of a personal computer. Phosphorescence spectra were obtained using a set of interference filters with transmission maxima at 1230, 1270, and 1310 nm. The phosphorescence kinetic curves were obtained by averaging the signal after a large number of exciting pulses, using the multichannel photon counting. The data were analyzed using the Microsoft Excel spreadsheets and Origin program (OriginLab corp.). The signal accumulation time did not exceed 30 min, and the average power of the exciting radiation varied from 4 to 41 mW. The experimental kinetic curves were approximated by the two-exponential function:

$$I(t) = I_0 [\exp(-t/\tau_{decay}) - \exp(-t/\tau_{rise})] \quad (1)$$

where $I(t)$ is the phosphorescence intensity in einsteins per second, I_0 is the pre-exponential factor and τ_{decay} and τ_{rise} are time-constants of the decay and rise phases.[31-33]

Results and Discussion

Absorption spectra

Absorption spectra of THPTS in all investigated solvents are indicated in Figure 1. They are similar in all media. The main absorption maxima are listed in Table 1. It was found that the absorption spectrum of THPTS, synthesized by Lyubimtsev's group coincides with that of Shastak's samples which were studied by our group previously (Table 1). The absorption spectra have four typical bacteriochlorin bands at about 372, 515, 760 nm and two typical chlorin bands at about 420 and 658 nm. Addition of 0.2 M SDS to aqueous media caused 2–3 nm shift of all bands to longer wavelengths and the 8–10% increase of both 650 and 760 nm bands, without appreciable change in the intensity ratio of these bands and the general shape of the absorption spectra. It is noteworthy, that most experiments reported in the present paper were done without the detergent. The dark red band at 760–762 nm is as strong as the violet band at 375 nm. The molar absorption coefficient at the maximum of the dark red band is exceptionally high ($\varepsilon = 1.4 \cdot 10^5$ $M^{-1}cm^{-1}$ [18,19]). The relative concentrations of chlorin and bacteriochlorin components were 1:5 in all samples.

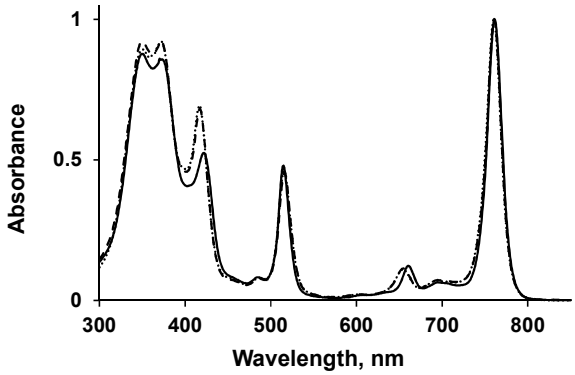

Figure. 1. Normalized absorption spectra of THPTS in 1 cm optical cell, in ethanol (solid line), deuterium oxide (dotted line) and water (dashed line). The concentration of the bacteriochlorin component is of 4.3–5.2 μM.

Table 1. Main absorption and fluorescence maxima (nm) and fluorescence quantum yields (Φ_f, for the bacteriochlorin component) of THPTS.

Solvent	Abs.	Fluor.	Φ_f
	Lyubimtsev's sample		
Ethanol	350, 373, 422, 515, 661, 761	665, 767	0.100 ± 0.005
D_2O	351, 372, 417, 515, 654, 760	662, 768	0.085 ± 0.005
H_2O	350, 372, 417, 516, 655, 761	661, 767	0.085 ± 0.005
H_2O with 0.2 M SDS	350, 375, 420, 516, 658, 763	665, 770	0.075 ± 0.005
	Shastak's sample		
Ethanol	350, 375, 423, 515, 661, 762	664, 766	0.110 ± 0.005
H_2O	350, 373, 418, 516, 655, 761	659, 766	0.080 ± 0.005

Fluorescence

The fluorescence spectra and excitation spectra of THPTS fluorescence in ethanol and aqueous media are shown in Figures 2 and 3. It follows from these figures that excitation at 375 nm causes fluorescence from both components of THPTS, since the absorption spectra of chlorin and bacteriochlorin components overlap at this wavelength (see also Figure 1). The main maxima and quantum yields of fluorescence are listed in Table 1. It follows from the fluorescence emission and fluorescence excitation spectra (Figure 3) that fluorescence of THPTS corresponds to the Q_y electronic transitions. The fluorescence bands at 659–663 and 766–768 nm belong to the (0-0) electronic transitions of the chlorin and bacteriochlorin components respectively.

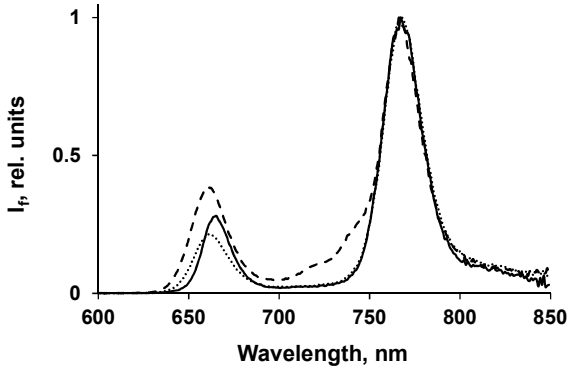

Figure 2. Normalized fluorescence spectra of THPTS in ethanol (solid line), deuterium oxide (dotted line) and water (dashed line) under excitation at 375 nm. I_f is the fluorescence intensity in einstein/s.

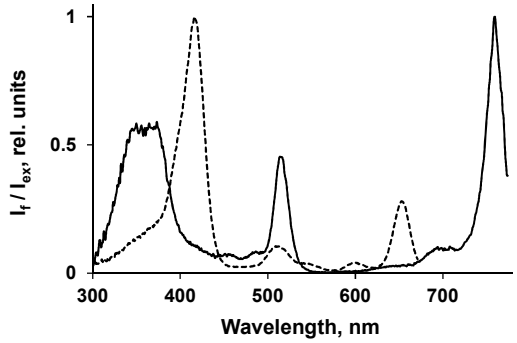

Figure 3. Normalized excitation spectra of THPTS fluorescence in water. Solid line – excitation spectrum of the bacteriochlorin component, fluorescence is detected at 780 nm. Dashed line – excitation spectrum of the chlorin component, fluorescence is detected at 680 nm. I_f and I_{ex} are the intensities of the fluorescence and excitation light, measured in einsteins per second, respectively. Absorbance is 0.19 at 760 nm.

If fluorescence is detected at 680 nm, which corresponds to the chlorin fluorescence, only chlorin bands are seen in the excitation spectrum (Figure 3). If fluorescence is detected at 780 nm, which corresponds to the fluorescence of bacteriochlorin, only bacteriochlorin excitation bands are seen (Figure 3).

The fluorescence yields of the bacteriochlorin component of THPTS $(\Phi_f)_{bcl}$ were obtained under excitation at 375 nm by comparison with fluorescence yield $(\Phi_f)_{ref}$ of TPPS in the same solvent using the following equation:

$$(\Phi_f)_{bcl} = (\Phi_f)_{ref}[(I_f)_{bcl}/I_{ex}(1–10^{-A})_{bcl}]/[(I_f)_{ref}/I_{ex}(1–10^{-A})_{ref}], \quad (2)$$

where I_f is the overall fluorescence intensity of bacteriochlorin and that of the reference (TPPS), A is absorbance of bacteriochlorin and TPPS at the excitation wavelength. It was found that the THPTS fluorescence yields are equal to 0.08–0.10 in all solvents.

Detailed studies of the chlorin fluorescence yield were not carried out since our main goal was investigation of the bacteriochlorin component. However, analysis of Figures 1–3 indicates that $(\Phi_f)_{cl}$ is roughly 1.5–2 fold higher.

It is noteworthy that the absorption and fluorescence spectra in all media are represented by series of similar distinct narrow bands. This fact indicates that molecules of THPTS are monomeric in both organic solvent (ethanol) and aqueous dispersions.

Trapping experiments

Figure 4 indicates that irradiation of pigment solutions by monochromatic light at 760 nm in the presence of DPIBF causes rapid bleaching of the main absorption maximum of the trap at 414 nm in aqueous solutions of THPTS containing 0.2 M SDS, which was added for solubilization of the trap. Similar results were obtained in D_2O and ethanol (data not shown). In the latter case, SDS was not added, since DPIBF is readily soluble in ethanol.

No bleaching of the bacteriochlorin component was observed during the irradiation time. Bleaching of the trap was not observed after irradiation of DPIBF solutions without THPTS by IR light. The obtained quantum yields are listed in Table 2. The data indicate that bacteriochlorin component of THPTS efficiently generate $^1O_2$ in both aqueous systems (D_2O and H_2O) and in organic solvent ethanol.

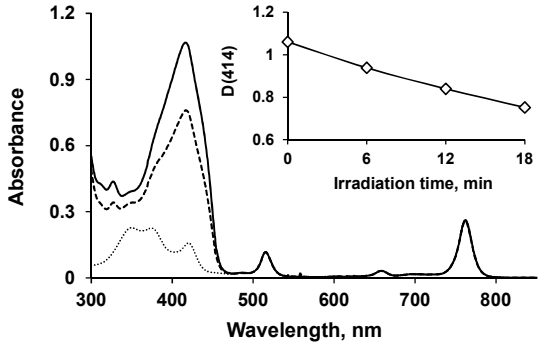

Figure 4. Absorption spectra of the mixture of THPTS (with 1.8 μM bacteriochlorin concentration) and DPIBF (39 μM) in water with 0.2 M SDS before (solid line) and after 18 min irradiation (dashed line) by monochromatic light of 760 nm, 55 μW. Inset shows the time course of the absorbance change at 414 nm under irradiation of the mixture at 760 nm. Dotted line indicates the absorption spectrum of THPTS in the mixture.

Table 2. Quantum yields of singlet oxygen generation (Φ_Δ) by the bacteriochlorin component of THPTS obtained using chemical trapping and detection of phosphorescence at 1270 nm.

Solvent	Chemical trapping by DPIBF, excitation at 760 nm	Phosphorescence, excitation at 395 nm
Ethanol	0.55 ± 0.05**	0.63 ± 0.06**
D_2O	0.65 ± 0.06*	0.45 ± 0.06**
H_2O	0.45 ± 0.05*	0.45 ± 0.06**,

*the data obtained in the presence of 0.2 M SDS, **no SDS was added.

IR phosphorescence measurements

In agreement with trapping experiments, we observed that excitation of THPTS solutions by violet LED (395 nm) causes the appearance of IR phosphorescence of oxygen at 1270 nm. The kinetic curves and spectra of phosphores-

cence arising after 1 μs excitation pulses at 395 nm in aerated solutions THPTS in ethanol, D_2O and H_2O are shown in Figures 5–7. All curves are bell-shaped. The rise phase reflects the rate of singlet oxygen formation due to energy transfer from the THPTS triplet state to oxygen, the decay phase corresponds to the rate of $^1O_2$ deactivation (see details in [30-33] and refs therein).

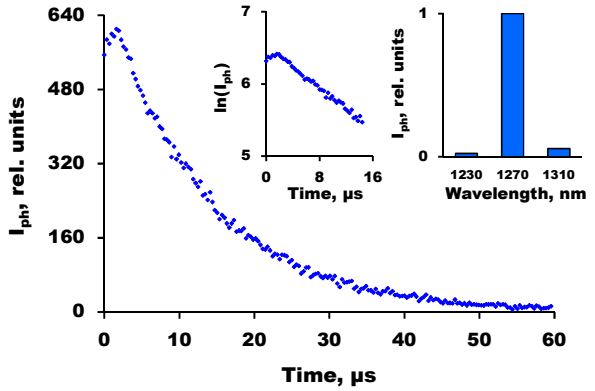

Figure 5. Normalized kinetic trace of $^1O_2$ phosphorescence at 1270 nm in aerated solutions of THPTS in ethanol recorded with 1.28 μs delay after the start of the exciting pulse using a time resolved photon counting method in Cartesian and semilogarithmic (inset) coordinates. Phosphorescence was excited at 395 nm in 10 mm quartz cell by 1 μs LED pulses with the 10 kHz repetition rate. Average excitation power was 11 mW, absorbance was 0.39 at the excitation wavelength. Acquisition time was 30 minutes. One channel dwell time was 320 ns. There was no bleaching of the 760 nm absorption band during the irradiation time. The concentration of the bacteriochlorin component was 6.1 μM. Left inset shows semilogarithmic plot of the kinetic trace, right inset indicates the phosphorescence spectrum measured with three interchangeable interference filters.

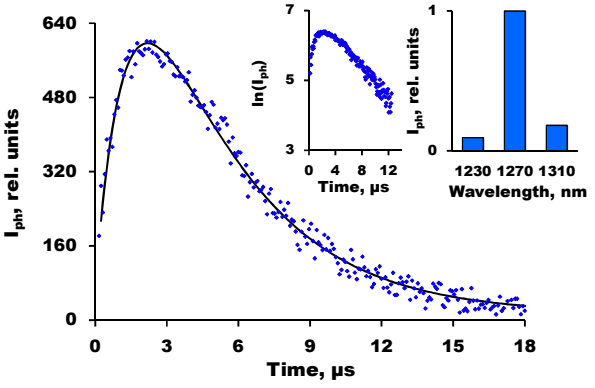

Figure 6. Normalized kinetic traces of $^1O_2$ phosphorescence at 1270 nm in aerated solutions of THPTS in distilled water in Cartesian and semilogarithmic (left inset), coordinates recorded with 1.12 μs delay after the start of the exciting pulse. Dots indicate experimental data, solid line is approximation by the Origin program. Phosphorescence was excited at 395 nm by 1 μs LED pulses with the 50 kHz repetition rate, average excitation power was 41 mW. Absorbance of the solution was ~ 0.42 at the excitation wavelength in 10 mm quartz cell. One channel dwell time was 80 ns. Accumulation time was 30 min (sum of phosphorescence from 15 solution portions with two minutes of irradiation). Bleaching of THTPS after 2 min irradiation was 15%. The initial concentration of the THTPS was 6.5 μM. Right inset is the phosphorescence spectrum.

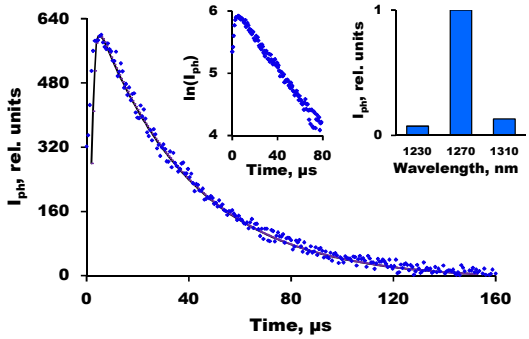

Figure 7. Normalized kinetic traces of $^1O_2$ phosphorescence at 1270 nm in aerated solutions of THTPS in Deuterium oxide in Cartesian and semilogarithmic (left inset) coordinates recorded with 1.28 μs delay after the start of the exciting pulse. Dots show experimental results. Solid line is approximation by the Origin program. Phosphorescence was excited at 395 nm by 1 μs LED pulses with the 5 kHz repetition rate, average excitation power was 6 mW. Absorbance of the solution was 0.41 at the excitation wavelength in 5 mm quartz cell. One channel dwell time was 640 ns. Accumulation time was 30 min (sum of phosphorescence from 3 solution portions after 10 minutes of irradiation). Bleaching of THTPS after 10 min irradiation was 12 %. Initial THTPS concentration was 12.5 μM. Right inset is the phosphorescence spectrum.

In ethanol (Figure 5), the rise time is known to be about 400 ns,[31,32] peak was observed at 1.5 μs. Since 2.7 μs after the excitation pulse, the decay becomes monoexponential with the decay time of 13 μs. With smaller THPTS concentration, the decay time increased to 13.5 μs which is equal to the $^1O_2$ lifetime in ethanol containing 4% water ([31,32] and refs therein). The emission maximum of the phosphorescence is at 1270 nm (right inset).

In H_2O and D_2O, the rise time of the kinetic curves was about 2 μs in both media, the peaks were observed at 2.5 and 6 μs correspondingly (Figures 6, 7). In water, the phosphorescence decay becomes exponential 10 μs after exciting pulse with the lifetime of about 3 μs that coincides with the $^1O_2$ lifetime in neat water.[31-34] In D_2O the decay time depended on the concentration of THPTS. With low THPTS concentration or in phenalenone solution, the decay time was close to 70 μs that coincides with the lifetime of $^1O_2$ in neat D_2O ([31,32] and refs therein). In the presence of 4.8 μM THPTS, the decay time was 54 μs. The increase in the THPTS concentration caused the decrease of the decay time. Application of the Stern-Volmer equation allowed us to estimate that the rate constant of $^1O_2$ quenching by THPTS is equal to 10^9 $M^{-1}s^{-1}$ (Figure 8).

Hence THPTS is capable of rather strong quenching of singlet oxygen. Similar property was previously found in solutions of bacteriochlorins of different structures.[7-11] Bacteriochlorophyll *a* is one of the strongest quenchers (see recent review[11]). Judging by our data, quenching activity of other porphyrins is much weaker.[35] Following the results of the paper,[35] it is likely that quenching of singlet oxygen by bacteriochlorins is due to formation of an intermediate charge transfer complex between $^1O_2$ and bacteriochlorin followed by energy dissipation:

$$^1O_2 + BChl \rightarrow (O_2^- \text{-- } BChl^+) \rightarrow {}^3O_2 + BChl + heat$$

More detailed studies of this process is out of the scope of the present work.

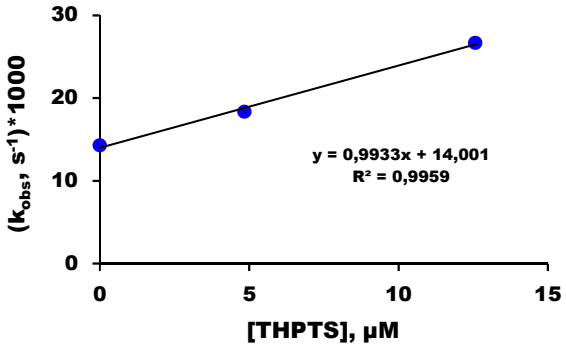

Figure 8. Stern-Volmer plot of the dependence of the phosphorescence decay rate (k_{obs}) after a LED pulses (395 nm) from the concentration of bacteriochlorin component of THPTS in D_2O, $k_q = (1.0\pm0.1)\times10^9$ $M^{-1}s^{-1}$).

Time resolved phosphorescence measurements allowed also estimation of the Φ_Δ for THPTS. The quantum yields were determined by comparison the total number of phosphorescence photons emitted by THPTS solutions $(I_p)_{tt}$ after the end of the excitation pulse (1 μs) with $(I_p)_{pn}$ (in einstein) emitted by phenalenone in the same solvents. The quantum yields of singlet oxygen generation by phenalenone is known to be 0.95±0.05.[36,37] Calculation were done according to the following equation:

$$(\Phi_\Delta)_{tt} = [(I_p)_{tt}/I_{ex}(1\text{-}10^{-A_{tt}})]/\ [(I_p)_{pn}/I_{ex}(1\text{-}10^{-A_{pn}}) \quad (3)$$

where A_{tt} and A_{pn} are absorbances of THPTS and phenalenone at the excitation wavelength (395 nm). The obtained quantum yields are listed in Table 2. It should be noted that $(\Phi_\Delta)_{tt}$ obtained using this equation is due to photosensitizing activities of both the bacteriochlorin and chlorin components of THPTS, which, as it follows from Figures 1 and 3, equally absorb light at 395 nm. It is known from literature sources that the quantum yields of $^1O_2$ in solutions of natural and synthetic chlorins and bacteriochlorins are rather similar. The reported values varied from 0.60 to 0.75 ([7,8,10,38-40] and refs therein). Whence, it is reasonable to propose that the obtained $(\Phi_\Delta)_{tt}$ corresponds to activities of both chlorin and bacteriochlorin components.

It is seen from Table 2, that the trapping and phosphorescence methods yield rather similar Φ_Δ values. The most accurate data were obtained using the trapping method since in the trapping experiments, power of the exciting light was very low (about 50 μW), at which there was no bleaching of the IR absorption band of THPTS during the irradiation time. Besides, the excitation wavelength corresponded to the main IR maximum of the absorption spectrum of the bacteriochlorin component.

In the phosphorescence experiments, the power of excitation was much higher (4–41 mW) that caused bleaching of the IR absorption band. Under conditions of our experiments (see experimental section) bleaching was not more than 15%. Simultaneously, a product absorbing at 395 nm appeared. It was difficult to accurately take all these factors into consideration. Nevertheless, the quantum yields obtained by trapping and phosphorescence methods were rather close.

Conclusions

Thus, our data provide unambiguous evidence that singlet oxygen is efficiently generated by THPTS in both aquatic environment and organic solvents. The quantum yields obtained in the present paper are close to those reported previously in methanol (Φ_Δ = 0.5),[17] acetonitrile (Φ_Δ = 0.75)[20] and ethanol (Φ_Δ = 0.5) as was obtained using Shastak's sample (see introduction). However, this result disagrees with the data of Riyad *et al.*[20] who could not detect $^1O_2$ in aqueous THPTS solutions. More precisely, Riyad et al. reported[20] that they have detected the phosphorescence of singlet oxygen in THPTS solution in acetonitrile, but could not observe it in aqueous solutions under the same conditions. As a result, they concluded "that the $^1O_2$ quantum yield in aqueous solutions of THPTS is 20-fold lower than in acetonitrile which is the detection limit of the employed setup".[20] Based on this fact, Riyad *et al.*[20] proposed that in water THPTS loses an ability to generate $^1O_2$ therefore, the photodynamic action of THPTS in water and living tissues proceeds solely via the free-radical Type I mechanism. It seems that the authors thought that the $^1O_2$ phosphorescence yields in different solvents depended on the quantum yield of $^1O_2$ formation only. However, it is common knowledge that the phosphorescence yield (Φ_{1270}) depends on several parameters besides Φ_Δ :[41,42]

$$\Phi_{1270} = \Phi_\Delta\, k_r \tau_\Delta \quad (4)$$

where k_r is the radiative rate constant of the $^1\Delta_g$ state and τ_Δ is the real lifetime of singlet oxygen in the used solvent. The values of k_r and τ_Δ have been studied by many researchers. See for instance, papers ([41-45] and refs therein). In particular, τ_Δ = 3.1 μs[33] and k_r = 0.209 s^{-1} in water.[43] In acetonitrile, τ_Δ = 59 μs,[46] k_r = 0.45 s^{-1}.[41] It follows from these values that the product ($k_r\tau_\Delta$) is equal to $0.65\cdot10^{-6}$ in water and $27\cdot10^{-6}$ in acetonitrile. Thus, the phosphorescence yield in water is 40-fold lower than in acetonitrile due to much lower values of the product $k_r\tau_\Delta$ in water. Riyad *et al.* correctly reported that the phosphorescence quantum yield (Φ_{1270}) in water is more than 20-fold smaller than in acetonitrile[20], but as mentioned above, it says nothing about the Φ_Δ value for THPTS. To obtain the correct Φ_Δ, one should compare the yields of $^1O_2$ phosphorescence in solutions of THPTS with that of a reference compound in the same solvent. Whence, the major argument of Riyad *et al.*,[20] has no real experimental basis. Our data suggest that $^1O_2$ generation by THPTS and the Type II mechanism are most probable steps of the THPTS photodynamic action in both aquatic and non aquatic environments. Besides, the involvement of THPTS in the Type I oxidation mechanism cannot be high, because as known from literature, the energy of the bacteriochlorin triplet state (1100 nm[47]) is much lower than that of triplet chlorophyll *a* (930 nm[48]). Therefore, the reactivity of triplet bacteriochlorin toward the cell components should be lower than that of triplet chlorophyll, reaction rate of which with lipids, aminoacids, proteins, nucleotides is known to be much lower that the reaction rates of $^1O_2$ with the same compounds ([49] and refs therein).

Acknowledgments. This work was performed with partial financial support from the Russian Science Foundation (Project # 23-65-10005, 2023).

References

1. Bonnett R. *J. Heterocyclic Chem.* **2002**, *39*, 455–470. DOI: 10.1002/jhet.5570390303
2. Mironov A.F. In: *Results of Science and Technology. Modern problems of laser physics. Vol. 3* (Akhmanov S.A., Chernyaeva V.B., Eds.) Moscow: VINITI **1990**, p. 5–62 [in Russian].
3. Lukyanets E.A. *Photodynamic Therapy and Photodiagnostics* **2013**, *2*, 3–16 [in Russian].
4. Abrahamse H., Hamblin M.R. *Biochem. J.* **2016**, *473*, 347–364. DOI: 10.1042/BJ20150942
5. Berezin D.B., Bondareva T.V., Shukhto O.V., Kustova T.V., Razgovorov P.B., Kustov A.V. *ChemChemTech (Izv. Vyssh. Uchebn. Zaved. Khim. Khim. Tekhnol.)* **2025**, *68*, 70–82. DOI: 10.6060/ivkkt.20256806.7166
6. Kustov A.V. *ChemChemTech (Izv. Vyssh. Uchebn. Zaved. Khim. Khim. Tekhnol.)* **2023**, *66*, 32–40. DOI: 10.6060/ivkkt.20236612.6902
7. Krasnovsky A.A. Jr. *Biophysics (Biofizika)* **1977**, *22*, 927–928 [in Russian].
8. Krasnovsky A.A. Jr. *Photochem. Photobiol.* **1979**, *29*, 29–36. DOI: 10.1111/j.1751-1097.1979.tb09255.x
9. Venediktov E.A., Krasnovsky A.A. Jr. *Zh. Prikl. Spektr. (J. Applied Spectroscopy, Minsk)* **1982**, *36*, 152–154.
10. Krasnovsky A.A. Jr., Vychegzhanina I.V., Drozdova N.N., Krasnovsky A.A. (senior). *Dokl. AN SSSR (Biophysics)* **1985**, *283*, 161–163.
11. Krasnovsky A.A. Jr., Benditkis A.S., Kozlov A.S. *Macroheterocycles* **2024**, *17*, 58–64. DOI: 10.6060/mhc245924k
12. Shastak S., Shulga A., Berr F., Wiedemann P. US patent 6410568 B1 **2002**.
13. Oertel M., Shastak S.I., Tannapfel A., Hermann R., Sack U., Moessner J., Berr F. *J. Photochem. Photobiol. B* **2003**, *71*, 1–10. DOI: 10.1016/S1011-1344(03)00091-5
14. Shastak S., Jean B., Handzel R., Kostenich G., Hermann R., Sack U., Orenstein A., Wang Y., Wiedemann P. *J. Photochem. Photobiol. B* **2005**, *78*, 203–213. DOI: 10.1016/j.jphotobiol.2004.11.006
15. Koifman O.I., Ponomarev G.V., Syrbu S.A., Zharov E.V., Sergeeva T.V., Lukovkin A.V. RF Patent 2535097 C1, **2013**.
16. Makarova E.A., Jakubovskaja R.I., Vorozhtsov G.N., Lastovoj A.P., Luk'janets E.A., Morozova N.B., Plotnikova E.A. RF Patent 2549953 C2, **2013**.
17. Dudkin S.V., Makarova E.A., Slivka L.K., Lukyanets E.A. *J. Porphyrins Phthalocyanines* **2014**, *18*, 107–114. DOI: 10.1142/S1088424613501162
18. Lyubimtsev A.V., Semeikin A.S., Koifman M.O., Koifman O.I. *Doklady Chemistry* **2023**, *508*, 13–22. DOI: 10.1134/S0012500823600128
19. Kishalova M.V., Zheglova N.V., Koifman M.O., Lyubimtsev A.V. *Macroheterocycles* **2024**, *17*, 190–196. DOI: 10.6060/mhc235562k
20. Riyad Y.M., Naumov S., Schastak S., Griebel J., Kahnt A., Haupl T., Neuhaus J., Abel B., Hermann R. *J. Phys. Chem. B* **2014**, *118*, 11646–11658. DOI: 10.1021/jp507270k
21. Gradyushko A.T., Sevchenko A.N., Solovyov K.N., Tsvirko M.P. *Photochem. Photobiol.* **1970**, *11*, 387–400. DOI: 10.1111/j.1751-1097.1970.tb06011.x
22. Kalyanasundaram K., Neumann-Spallart M. *J. Phys. Chem.* **1982**, *86*, 5163–5169. DOI: 10.1021/j100223a022
23. Foote C.S., Wuesthoff M.T., Wexler S., Burstain I.G., Denny R., Schenck G.O., Schulte-Elte K-H. *Tetrahedron* **1967**, *23*, 2583–2599. DOI: 10.1016/0040-4020(67)85123-8
24. Krasnovsky A.A. Jr., Kozlov A.S., Roumbal Y.V. *Photochem. Photobiol. Sci.* **2012**, *11*, 988–997. DOI: 10.1039/c2pp05350k
25. Krasnovsky A.A., Kozlov A.S. *J. Photochem. Photobiol. A* **2016**, *329*, 167–174. DOI: 10.1016/j.jphotochem.2016.06.026
26. Holmberg K. In: *Surfactants. Ullmann's Encyclopedia of Industrial Chemistry*. Weinheim: Wiley-VCH **2019**, p. 1–56. DOI: 10.1002/14356007.a25_747.pub2
27. Malliaris A., Binana W. *J. Colloid Interface Sci.* **1984**, *102*, 305–330. DOI: 10.1016/0021-9797(84)90227-3
28. Wilkinson F., Helman W.P., Ross A.B. *J. Phys. Chem. Ref. Data* **1993**, *22*, 113–262. DOI: 10.1063/1.5559333
29. Tanielian C., Wolff C., Esch M. *J. Phys. Chem.* **1996**, *100*, 6555–6560. DOI: 10.1021/jp952107s
30. Krasnovsky A.A., Benditkis A.S., Kozlov A.S. *Biochemistry (Moscow)* **2019**, *84*, 153–163. DOI: 10.1134/S0006297919020068
31. Krasnovsky A.A. Jr. *J. Photochem. Photobiol. A* **2008**, *196*, 210–218. DOI: 10.1016/j.jphotochem.2007.12.015
32. Krasnovsky A.A. Jr. *Physics of Wave Phenomena* **2020**, *28*, 116–134. DOI: 10.3103/S1541308X20020090
33. Egorov S.Yu., Kamalov V.F., Koroteev N.I., Krasnovsky A.A. Jr., Toleutaev B.N., Zinukov S.V. *Chem. Phys. Lett.* **1989**, *163*, 421–424. DOI: 10.1016/0009-2614(89)85161-9
34. Lepeshkevich S.V., Stasheuski A.S., Parkhats M.V., Galievsky V.A., Dzhagarov B.M. *J. Photochem. Photobiol. B* **2013**, *120*, 130–141. DOI: 10.1016/j.jphotobiol.2012.12.012
35. Krasnovsky Jr. A.A., Venediktov E.A., Chernenko O.M. *Biophysics (Biofizika)* **1982**, *27*, 1009–1016.
36. 36. Oliveros E., Suardi-Murasecco P., Aminian-Saghafi T., Braun A.M., Hansen H.-J. *Helv. Chim. Acta* **1991**, *74*, 79–90. DOI: 10.1002/hlca.19910740110
37. Schmidt R., Tanielian C., Dunsbach R., Wolff C. *J. Photochem. Photobiol. A* **1994**, *79*, 11–17. DOI: 10.1016/1010-6030(93)03746-4
38. Kochubeev G.A., Frolov A.A., Gurinovich G.P. *Khim. Fizika* **1989**, *8*, 1184–1190 [in Russian].
39. Zenkevich E., Sagun E., Knyukshto V., Shulga A., Mironov A., Efremova O., Bonnett R., Songca S.P., Kassem M. *J. Photochem. Photobiol. B* **1996**, *33*, 171–180. DOI: 10.1016/1011-1344(95)07241-1
40. Bonnett R., Charlesworth P., Djelal B.D., Foley S., McGarvey D.J., Truscott T.G. *J. Chem. Soc., Perkin Trans.* **1999**, *2*, 325-328. DOI: 10.1039/A805328F
41. Krasnovsky A.A. Jr. *Chem. Phys. Lett.* **1981**, *81*, 443–445. DOI: 10.1016/0009-2614(81)85647-3
42. Krasnovsky A.A. Jr. *Membr. Cell Biology* **1998**, *12*, 665–690. PMID: 10379647
43. Hild M., Schmidt R. *J. Phys. Chem. A* **1999**, *103*, 6091–6096. DOI: 10.1021/jp9906942
44. Minaev B.F. *Russ. Chem. Rev.* **2007**, *76*, 988–1010. DOI: 10.1070/RC2007v076n11ABEH003720
45. Dzhagarov B.M., Zharnikova E.S., Galievsky V.A., Stasheuski A.S., Parkhats M.V. *Russian Physics Journal* **2022**, *64*, 2008–2016. DOI: 10.1007/s11182-022-02550-3
46. Rodgers M.A.J. *J. Am. Chem. Soc.* **1983**, *105*, 6201–6205. DOI: 10.1021/ja00358a001
47. Takiff L., Boxer S.G. *J. Am. Chem. Soc.* **1988**, *110*, 4425–4426. DOI: 10.1021/ja00221a059
48. Krasnovsky A.A. Jr., Kovalev Yu.V. *Biochemistry (Moscow)* **2014**, *79*, 349–361. DOI: 10.1134/S000629791404004X
49. Krasnovsky A.A. Jr. *Proc. Roy. Soc, Edinburg B* **1994**, *102*, 219–235. DOI: 10.1017/S0269727000014147

Received 05.09.2025
Accepted 01.10.2025